

# OPTIMIZATION OF A 2-MICRON LASER FREQUENCY STABILIZATION SYSTEM FOR A DOUBLE-PULSE CO<sub>2</sub> DIFFERENTIAL ABSORPTION LIDAR

Songsheng Chen<sup>1</sup>, Jirong Yu<sup>2</sup>, Yingxin Bai<sup>1</sup>, Grady Koch<sup>2</sup>, Mulugeta Petros<sup>3</sup>,  
Bo Trieu<sup>2</sup>, Paul Petzar<sup>4</sup>, Upendra N. Singh<sup>2</sup>, Michael J. Kavaya<sup>2</sup>, Jeffrey Beyon<sup>2</sup>

<sup>1</sup>SSAI, One Enterprise Parkway, Suite 200, Hampton, VA 23666 USA

757-864-1105, songsheng.chen-1@nasa.gov

<sup>2</sup>NASA Langley Research Center, MS 474, Hampton, VA 23681 USA

<sup>3</sup>STC, 10 Basil Sawyer Drive, Hampton, VA 23666 USA

<sup>4</sup>National Institute of Aerospace, Hampton, VA 23666 USA

## ABSTRACT

A carbon dioxide (CO<sub>2</sub>) Differential Absorption Lidar (DIAL) for accurate CO<sub>2</sub> concentration measurement requires a frequency locking system to achieve high frequency locking precision and stability. We describe the frequency locking system utilizing Frequency Modulation (FM), Phase Sensitive Detection (PSD), and Proportional Integration Derivative (PID) feedback servo loop, and report the optimization of the sensitivity of the system for the feed back loop based on the characteristics of a variable path-length CO<sub>2</sub> gas cell. The CO<sub>2</sub> gas cell is characterized with HITRAN database (2004). The method can be applied for any other frequency locking systems referring to gas absorption line.

## 1. INTRODUCTION

Active sensing of carbon dioxide (CO<sub>2</sub>) in the atmosphere, such as a pulsed Differential Absorption Lidar (DIAL) or a continuous wave Laser Absorption Spectrometer (LAS), has become a very promising technique for accurate measurement of the CO<sub>2</sub> concentration, which has a significant contribution to the global warming and climate change. The active sensing of the CO<sub>2</sub> concentration promises a full day and night coverage during all seasons and a quantitative study of CO<sub>2</sub> surface sources and sinks [1]. Similar to all the pulsed differential absorption lidars, a double-pulsed 2-micron differential absorption lidar CO<sub>2</sub> under development requires frequency-stabilized and narrow linewidth continuous wave (CW) seeder lasers as injection seeding sources. It has been theoretically estimated that the frequency variation for the CO<sub>2</sub> differential absorption lidar at 2 micron has to be within ~2 MHz, or frequency stability has to be less than ~1E-8, to achieve CO<sub>2</sub> concentration with the accuracy of one ppm [2].

## 2. BASIC PRINCIPLE AND THEORY

### 2.1 Frequency modulation

The single frequency 2-micron laser beam is directed into a single frequency modulator made of MgO:LiNbO<sub>3</sub> and the output laser beam is modulated.

In case of a simple sine-wave modulation, the modulation signal is given,

$$m\{t\} = m_0 \sin\{2\pi v_m t + \varphi_m\} \quad (1)$$

where  $m_0$ ,  $v_m$ , and  $\varphi_m$  are the amplitude, frequency, and initial phase of the harmonic modulation signal respectively.

The electric field of the laser beam from the frequency modulator, can be expressed,

$$E\{t\} = E_0 \exp\{i(\pi v_c t + \varphi_0 + M \sin\{2\pi v_m t + \varphi_m\})\} + c.c. \quad (2)$$

where  $E_0$ ,  $v_c$ , and  $\varphi_0$  are the amplitude, frequency, and initial phase of the laser carrying beam respectively ( $v_m \ll v_c$ ).  $M$  is the modulation index related to the amplitude, the frequency, and the efficiency of the modulation. Under a normal weak modulation, or  $M \ll 1$ , the  $E\{t\}$  in (2) can be expanded as a Fourier series,

$$\begin{aligned} E\{t\} &= \frac{E_0}{2} \sum_{n=-\infty}^{+\infty} J_n\{M\} \exp\{i(2\pi(v_c + n v_m)t + \varphi_0 + n\varphi_m)\} + c.c. \\ &\approx \frac{E_0}{2} J_0\{M\} \exp\{i(2\pi v_c t + \varphi_0)\} \\ &+ \frac{E_0}{2} J_1\{M\} \{ \exp\{i(2\pi(v_c + v_m)t + \varphi_0 + \varphi_m)\} \\ &- \exp\{i(2\pi(v_c - v_m)t + \varphi_0 - \varphi_m)\} \} + c.c. \\ &= \frac{E_0}{2} \exp\{i(2\pi v_c t + \varphi_0)\} \\ &+ \frac{E_0}{2} \frac{M}{2} \{ \exp\{i(2\pi(v_c + v_m)t + \varphi_0 + \varphi_m)\} \\ &- \exp\{i(2\pi(v_c - v_m)t + \varphi_0 - \varphi_m)\} \} + c.c. \end{aligned} \quad (3)$$

where  $J_n\{M\}$  is Bessel Function (first kind and integer order  $n$ ) and the terms of order  $M^2$  and higher are dropped.

To lock the laser frequency to the center of a specified CO<sub>2</sub> gas absorption line, the modulated laser beam is directed into a variable path-length CO<sub>2</sub> gas cell and the laser frequency is tunable within the width of the CO<sub>2</sub> gas absorption line with a driving of the feedback servo loop. The wavelength of the CO<sub>2</sub> absorption line is 2.050967 μm.

## 2.2 CO<sub>2</sub> gas cell

For optimization of the frequency locking purposes, a variable pass-length CO<sub>2</sub> gas cell is used and the gas in the cell is refillable to different pressures. For the frequency-locking purpose, the CO<sub>2</sub> gas cell is characterized in amplitude attenuation,  $\delta$ , and phase shift,  $\varphi$ , similar to a frequency modulation spectroscopy [3], due to the resonant absorption and resonant dispersion at the specified absorption line. The  $\delta$  and  $\varphi$  are defined for three frequencies,  $(\nu_c - \nu_m)$ ,  $\nu_c$ , and  $(\nu_c + \nu_m)$  as

$$\begin{aligned} \delta_c &= \frac{\alpha_c L}{2}; & \varphi_c &= \frac{2\pi\nu_c n_c L}{c}; \\ \delta_{c\pm m} &= \frac{\alpha_{c\pm m} L}{2}; & \varphi_{c\pm m} &= \frac{2\pi\nu_{c\pm m} L}{c}(\nu_c \pm \nu_m); \end{aligned} \quad (4)$$

where  $c$  is the speed of light,  $\alpha_{c-m}$ ,  $\alpha_c$ , and  $\alpha_{c+m}$ , are intensity absorption coefficients and  $n_{c-m}$ ,  $n_c$ , and  $n_{c+m}$ , are indexes of refraction for the laser beams at three different frequencies. The intensity absorption coefficients and the indexes of refraction are directly related to the specified absorption line shape of the CO<sub>2</sub> gas in the cell. The electric field of the beam after passing through the cell can be expressed by,

$$\begin{aligned} E\{t\} &= \frac{E_0}{2} \exp\{-i(\delta_c + i\varphi_c)\} \exp\{i(2\pi\nu_c t + \varphi_0)\} \\ &+ \frac{E_0 M}{2} \{\exp\{-i(\delta_{c+m} + i\varphi_{c+m})\} \exp\{i(2\pi(\nu_c + \nu_m)t + \varphi_0 + \varphi_m)\} \\ &- \exp\{-i(\delta_{c-m} + i\varphi_{c-m})\} \exp\{i(2\pi(\nu_c - \nu_m)t + \varphi_0 - \varphi_m)\}\} + c.c. \end{aligned} \quad (5)$$

The intensity of laser beam to be detected is

$$\begin{aligned} I\{t\} &= \frac{c}{8\pi} |E\{t\}|^2 = \frac{c}{8\pi} E\{t\} E^*\{t\} \\ &\approx \frac{c}{8\pi} (E_0)^2 \frac{1}{2} \exp\{-2\delta_c\} \{1 + \cos(4\pi\nu_c t + 2\varphi_0 - 2\varphi_c)\} \\ &+ M \exp\{\delta_c - \delta_{c+m}\} \cos(2\pi\nu_m t + \varphi_c + \varphi_m - \varphi_{c+m}) \\ &+ M \exp\{\delta_c - \delta_{c-m}\} \cos(2\pi\nu_m t + \varphi_c + \varphi_m - \varphi_{c-m}) \\ &+ \frac{M}{2} \exp\{\delta_c - \delta_{c+m}\} \cos(2\pi(2\nu_c + \nu_m)t + 2\varphi_0 + \varphi_m - \varphi_c - \varphi_{c+m}) \\ &+ \frac{M}{2} \exp\{\delta_c - \delta_{c-m}\} \cos(2\pi(2\nu_c - \nu_m)t + 2\varphi_0 + \varphi_m - \varphi_c - \varphi_{c-m}) \end{aligned} \quad (6)$$

where the terms of order  $M^2$  are ignored due to  $M \ll 1$ .

Generally, a photo-detector can only response to signals from zero to radio frequency (rf), including modulation frequency, so the terms,  $\nu_c$ ,  $2\nu_c - \nu_m$ ,  $2\nu_c + \nu_m$ , are averaged to a direct current (dc) signal. The detected signal is proportional to the intensity of the laser beam and can be separated into two signals; one is a dc signal and the other a signal at modulation frequency. The output current signal from the photo-detector at the

modulation frequency is more interesting for a phase sensitive detection and can be expressed by

$$\begin{aligned} S_{\text{mod}}\{t\} &\propto \frac{c}{8\pi} (E_0)^2 \frac{M}{2} \{\mathcal{F}_{\text{cos}} \cos(2\pi\nu_m t + \varphi_m) - \mathcal{F}_{\text{sin}} \sin(2\pi\nu_m t + \varphi_m)\} \\ \mathcal{F}_{\text{cos}} &= \exp\{-2\delta_c\} \{\exp\{\delta_c - \delta_{c+m}\} \cos(\varphi_c - \varphi_{c+m}) \\ &+ \exp\{\delta_c - \delta_{c-m}\} \cos(\varphi_c - \varphi_{c-m})\} \\ \mathcal{F}_{\text{sin}} &= \exp\{-2\delta_c\} \{\exp\{\delta_c - \delta_{c+m}\} \sin(\varphi_c - \varphi_{c+m}) \\ &+ \exp\{\delta_c - \delta_{c-m}\} \sin(\varphi_c - \varphi_{c-m})\} \end{aligned} \quad (7)$$

or

$$S_{\text{mod}}\{t\} = C_{\text{det}} M \{\mathcal{F}_{\text{cos}} \cos(2\pi\nu_m t + \varphi_m) - \mathcal{F}_{\text{sin}} \sin(2\pi\nu_m t + \varphi_m)\} \quad (8)$$

where  $C_{\text{det}}$  is a constant of the photo-detector and related to the optical power incident on the photo-detector, the quantum efficiency, the area, and gain of the photo-detector, as well as the energy of the modulation wave. The terms,  $\mathcal{F}_{\text{cos}}$  and  $\mathcal{F}_{\text{sin}}$ , are determined by the specified absorption line and the line shape of the CO<sub>2</sub> gas in the cell.

## 2.3 Phase sensitive detection

Phase sensitive detection technique is an effective way to recover the small signal buries in larger ambient noises by narrow bandwidth amplification. It requires a phase sensitive detector, or lock-in amplifier, to realize extremely narrow bandwidth detection, normally  $1e^{-3}$  Hz, through a phase-locked loop. By multiplying a local reference signal,  $S_L\{t\} = S_0 \cos(2\pi\nu_L t + \varphi_L)$ , where  $S_0$ ,  $\nu_L$ , and  $\varphi_L$  are the amplitude, frequency, and phase of the local reference signal respectively, on the photo-detector signal, equation (8), and applying a low-pass filter to the multiplied signal, a phase-sensitive dc signal is achieved especially when  $\nu_L = \nu_m$ ,

$$S_{\text{psd}} = \frac{1}{2} C_{\text{det}} M S_0 \{\mathcal{F}_{\text{cos}} \cos(\varphi_L - \varphi_m) + \mathcal{F}_{\text{sin}} \sin(\varphi_L - \varphi_m)\} \quad (9)$$

Typically,

$$S_{\text{psd}} = S_1 = \frac{1}{2} C_{\text{det}} M S_0 \mathcal{F}_{\text{cos}}; \quad \varphi_L - \varphi_m = 0 \quad (10)$$

$$S_{\text{psd}} = S_2 = \frac{1}{2} C_{\text{det}} M S_0 \mathcal{F}_{\text{sin}}; \quad \varphi_L - \varphi_m = \frac{\pi}{2}$$

These dc signals are directly proportional to the amplitude of the detected modulation signal and can be used to lock the frequency of the laser beam based on  $\mathcal{F}_{\text{cos}}$  and  $\mathcal{F}_{\text{sin}}$ , the characteristics of CO<sub>2</sub> absorption line. Phase dependency of the phase-sensitive dc signal, in case of  $\varphi_L - \varphi_m \neq 0, \frac{\pi}{2}$ , can be eliminated by a so-called dual-phase lock-in technique, in which another local reference signal,  $S'_L\{t\} = S_0 \sin(2\pi\nu_L t + \varphi_L)$ ,

which has only a phase shift of  $\frac{\pi}{2}$  from the first one, is applied to photo-detector signal, equation (8), separately. The second PSD signal is,

$$S'_{psd} = \frac{1}{2} C_{det} M S_0 \{F_{\cos} \sin(\varphi_L - \varphi_m) - F_{\sin} \sin(\varphi_L - \varphi_m)\} \quad (11)$$

so the dual-phase lock-in signal, which eliminates the phase dependency, will be,

$$S = \sqrt{(S_{psd})^2 + (S'_{psd})^2} \quad (12)$$

## 2.4 Calculation of $S_1, S_2, S$

For the purposes of comparison and optimization of our current frequency-locking system [4], the calculation is limited to a modulation frequency of 175 MHz. A Gaussian absorption line shape is a good approximation of the characteristics of the CO<sub>2</sub> gas cell with a pressure of several Torres and a variable length of 6 to 12 meters. The normalized amplitude attenuation at the specified CO<sub>2</sub> absorption line and the related phase shift can be expressed by [5],

$$\delta\{\nu\} = \exp\{-\ln(2) \frac{\nu^2}{(\Delta\nu_D)^2}\}$$

$$\varphi\{\nu\} = -\frac{2}{\sqrt{\pi}} \exp\{-\ln(2) \frac{\nu^2}{(\Delta\nu_D)^2}\} \int_0^{\frac{\nu\sqrt{\ln(2)}}{\Delta\nu_D}} \exp(-\xi^2) d\xi \quad (13)$$

where  $\nu$  is relative frequency shifted from the center frequency of the specified CO<sub>2</sub> absorption line and  $\Delta\nu_D$  is the full width half maximum (FWHM) of the specified CO<sub>2</sub> absorption line. A typical normalized amplitude attenuation line with a full width half maximum of 350MHz,  $\Delta\nu_D=350$ MHz, and the related phase shift are shown in Fig.1.

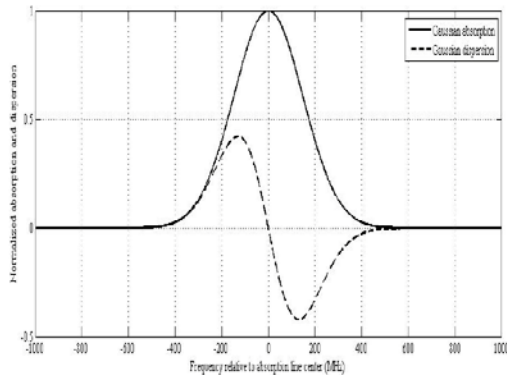


Fig. 1. Typical Gaussian absorption and dispersion with a full width half maximum of 350MHz

Fig.2 shows the calculated PSD signals,  $S_1, S_2, S$  for different line width of the absorption line, which can be

obtained by changing the pressure and length of the CO<sub>2</sub> absorption cell.

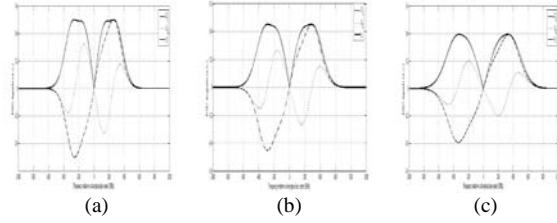
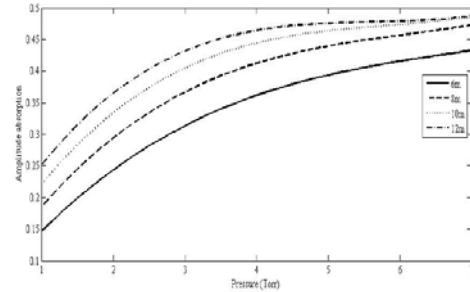


Fig. 2. Calculated PSD signals for different absorption line widths referring to the modulation frequency, (a)  $\nu_m/\Delta\nu_D=0.4$ , (b)  $\nu_m/\Delta\nu_D=0.5$ , (c)  $\nu_m/\Delta\nu_D=0.6$

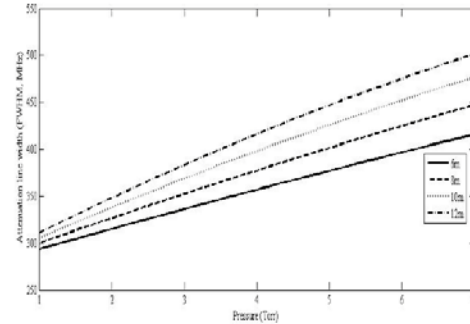
Both  $S_1$  and  $S_2$  signals around the center of absorption line can be utilized as error signals of the PID feedback servo loop for the frequency locking. The sensitivity for a certain detection and feed back servo loop system depends on the slope of the signals,  $S_1$  or  $S_2$ , around the center of absorption line.

## 3. SENSITIVITY ANALYSIS OF THE FEED BACK LOOP

Practically both the amplitude attenuation and the line width of the gas absorption line vary when the pressure of the gas cell changes. The variable pass-length CO<sub>2</sub> gas cell is characterized with HITRAN database (2004) and shown in Fig. 3.



(a)



(b)

Fig. 3. Amplitude attenuation (a) and line width (b) of the CO<sub>2</sub> absorption line for different path-length of the gas cell as a function of the pressure in the gas cell

The slopes of the PSD signals,  $S_1$  and  $S_2$  around the center of the absorption line present the sensitivity of the feed back loop to drive the frequency of the laser frequency and are calculated within a range of  $\pm 5$  MHz at the center. These calculated results are shown in Fig. 4.

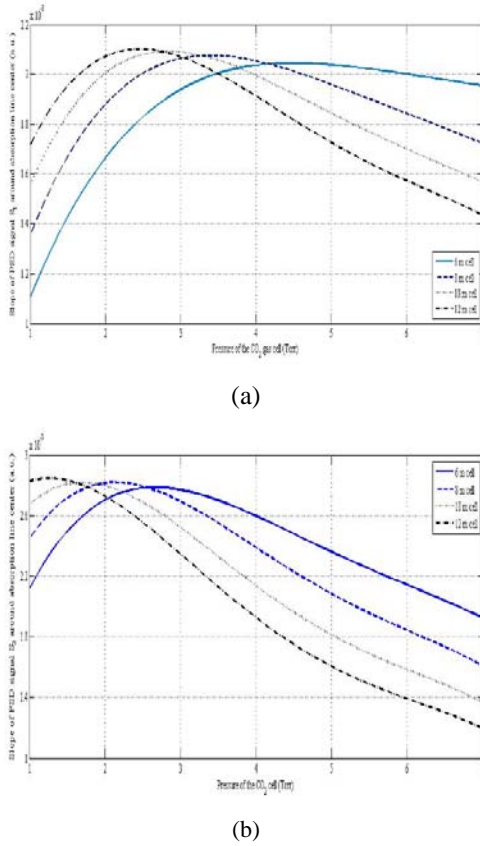


Fig. 4. Calculated PSD signals,  $S_1$  (a) and  $S_2$  (b) around center of the  $\text{CO}_2$  absorption line for different path-length of the gas cell as a function of the pressure in the gas cell

Both PSD signals,  $S_1$  and  $S_2$ , show the optimized sensitivities at different pressures of the gas cell can be obtained for different lengths of the cell.

#### 4. EXPERIMENT

The verification of the experiment has been set up and the diagram of the experiment and displays of the results are shown in Fig. 5.

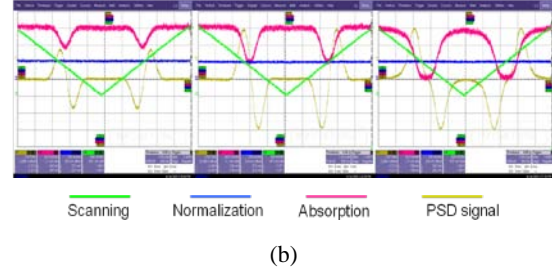
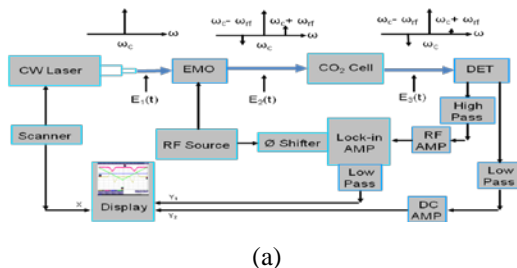


Fig. 5. (a) Diagram of the experiment for verification of the optimization of the frequency-locking system; (b) PSD signal ( $S_2$ ) and absorption of the specified  $\text{CO}_2$  line for a 8-m fixed length of the gas cell at different pressures, 1.5 Torr (left), 3.0 Torr (middle), 7.0 Torr (right).

The PSD signal,  $S_2$ , at the pressure of 3.2 Torr was chosen for the frequency locking and the frequency variation of less than 1 MHz was achieved and will be reported separately in details.

#### 5. CONCLUSIONS

The optimization of a 2-micron laser frequency locking system with a FM, PSD, and PID feedback servo loop has been simulated and verified in terms of characteristics of the  $\text{CO}_2$  gas absorption cell. The results of the simulations can be applied to any other frequency locking system referring to a gas absorption line.

#### REFERENCES

- [1] Jerome Caron and Yannig Durand, 2009: Operating wavelengths optimization for a spaceborne lidar measuring atmospheric  $\text{CO}_2$ , *Appl. Opt.*, **48**, No. 28, pp. 5413-5422
- [2] E. Ehret, C. Kiemle, M. Wirth, A. Amediek, A. Fix, and S. Houweling, 2008: Space-borne remote sensing of  $\text{CO}_2$ ,  $\text{CH}_4$ , and  $\text{N}_2\text{O}$  by integrated path differential absorption lidar: a sensitivity analysis, *Appl. Phys. B*, **90**, pp. 593-608.
- [3] G. C. Bjorklund and M. D. Levenson, 1983: Frequency Modulation (FM) Spectroscopy, *Appl. Phys. B*, **32**, pp. 145-152.
- [4] G. J. Koch, J. Y. Beyon, F. Gibert, B. W. Barnes, S. Ismail, M. Petros, P. J. Petzar, J. Yu, E. A. Modlin, K. J. Davis, and U. N. Singh, 2008: Side-line tunable laser transmitter for differential absorption lidar measurements of  $\text{CO}_2$ : design and application to atmospheric measurements, *Appl. Opt.*, **47**, No. 7, pp. 944-956.
- [5] S. W. North, X. S. Zheng, R. Fei, and G. E. Hall, 1996: Line shape analysis of Doppler broadened frequency-modulated line spectra, *J. Chem. Phys.*, **104**, No. 6, pp. 2129-2135.